ELSEVIER

Chemical Engineering Journal 76 (2000) 247–252

Chemical Engineering Journal

www.elsevier.com/locate/cej

Short communication

Liquid-solid mass transfer behaviour of rotating screen discs

G.H. Sedahmed *, M.Z. Al-Abd, Y.A. El-Taweel, M.A. Darwish

Chemical Engineering Department, Faculty of Engineering, Alexandria University, Alexandria, Egypt

Received 17 March 1999; received in revised form 10 October 1999; accepted 20 October 1999

Abstract

Rates of mass transfer at rotating single horizontal screen disc and rotating stacks of closely packed and separated screens were studied by measuring the limiting current for the cathodic reduction of ferricyanide ions. Variables studied were screen rotation speed, mesh number of the screen, physical properties of the solution, number of screens per stack, screen separation and the effect of superimposed axial flow. Mass transfer data at single rotating screen disk were correlated by the following equation which is based on the surface renewal model

$$J = 0.26\,\mathrm{Re}^{-0.5}\left(\frac{r}{d_w}\right)^{0.5}.$$

Mass transfer rates at rotating closely packed screen bed were found to decrease below the single screen value by an amount ranging from 20 to 43.6% depending on rotation speed, mesh number and number of screens per bed. Superimposed axial flow was found to increase the rate of mass transfer at rotating screens especially at $\mathrm{Re_f}$>1095. Implications of the present results for the design of high space time yield electrochemical reactors and catalytic reactors were noted.

Keywords: Mass transfer; Electrochemical reactor; Rotating screen disc

1. Introduction

The use of screens and expanded metals in building electrochemical and catalytic reactors used to conduct diffusion controlled heterogeneous reactions is receiving a growing interest in view of their high turbulence promoting ability and their high specific area. Previous studies on enhancing the rate of mass transfer at screens have included single phase flow [1–4], two phase flow [5], gas sparging [6,7], counter-electrode gas stirring [8] and vibration [9,10]. The object of the present work is to study the rate of mass transfer at horizontal rotating screen disc. To this end, the electrochemical technique which involves measuring the limiting current of the cathodic reduction of ferricyanide ion was used [11]. The technique has the advantage that the screen surface remains unaltered during measurements.

A continuous electrochemical reactor employing and array of solid rotating discs mounted on a rotating vertical shaft as a working electrode has been recently studied and found promising [12–14]. It is hoped that the performance of such a reactor could be improved by replacing the rotating discs by rotating screens. Also rotating screens could be used in building catalytic reactors where the catalyst is deposited on the screen surface. Although no previous studies on rotating screen disc have been reported, some work has been reported on solid rotating disc. Levich [15] derived the following equation for a rotating disc under laminar flow conditions in an infinite medium.

$$\mathrm{Sh} = 0.62\,\mathrm{Sc}^{0.33}\ \mathrm{Re}^{0.5} \quad (1)$$

The data obtained by Lehmkuhl and Hudson [16] for a disc rotating in a cylindrical cavity under laminar flow by using the dissolution of cinamic acid in water could be correlated by the equation [17],

$$\mathrm{Sh} = 0.43\,\mathrm{Re}^{0.5}\,\mathrm{Sc}^{0.33} \quad (2)$$

Langlois et al. [17] who studied the rate of mass transfer at a disc rotating in a small diameter cylindrical container under laminar flow conditions using the electrochemical technique correlated their data by the equation

$$\mathrm{Sh} = 0.47\,\mathrm{Re}^{0.5}\,\mathrm{Sc}^{0.33} \quad (3)$$

* Corresponding author.

1385-8947/00/$ – see front matter
PII: S1385-8947(99)00172-2

For turbulent flow, mass transfer data at rotating discs were correlated for the range $2.7\times10^5<\mathrm{Re}<1.5\times10^6$ by the equation [11]

$$\mathrm{Sh} = 0.0007\ \mathrm{Re}^{0.9}\ \mathrm{Sc}^{0.33} \quad (4)$$

2. Experimental technique

The apparatus (Fig. 1) consisted of the cell and electrical circuit. The cell consisted of a plexiglass cylinder of 5.5 cm diameter and 30 cm height. The cathode was 5 cm diameter nickel plated stainless single screen or number of screens fixed horizontally at the center to a vertical stainless steel stem of 3 mm diameter. The stem which acted as a screen holder and current feeder was isolated by epoxy except at the contact with the screen. The upper end of the stem was connected to the shaft of a variable speed motor through a plastic sleeve. The lower end of the stem resided in a smooth cylindrical cavity of 3.5 mm diameter machined in a teflon disc fixed at the cell bottom where the stem can rotate freely in the cavity. A stainless steel cylindrical sheet of 30 cm height lining the cell wall was used as anode. The anode area was higher than the highest cathode area, the ratio between anode area and cathode area ranged from 1.85 to 15.4 depending on the number of screens per cathode and screen mesh number and wire diameter. The high anode/cathode area ratio assured that the limiting current would be reached first at the cathode and no oxygen evolution would take place at the anode.

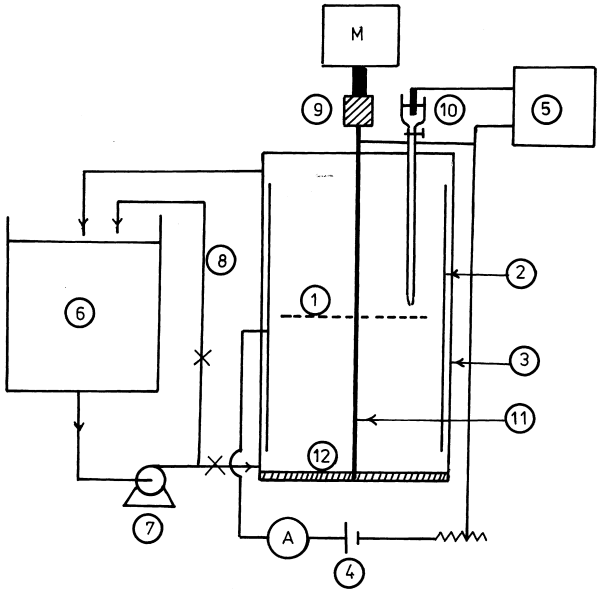

Fig. 1. Apparatus: 1, rotating screen cathode; 2, cylindrical stainless steel anode; 3, plexiglass column; 4, dc power supply; 5, potentiometer; 6, plexiglass storage tank; 7, plastic centrifugal pump; 8, by pass; 9, plastic sleeve; 10, Luggin tube with a reference electrode; 11, screen holder and current feeder; 12, fixed Teflon disc with a central cavity.

To test the effect of solution flow, the cell was fitted with a plexiglass solution inlet tube and a solution outlet tube at its bottom and top respectively. Solution was circulated between 20 l plexiglass storage tank and the cell by means of a plastic centrifugal pump.

The electrical circuit consisted of 10 V d.c. power supply with a voltage regulator, a multirange ammeter and the cell. Polarization curves from which the limiting current was obtained were plotted by increasing the current stepwise and measuring the corresponding cathode potential against a reference electrode by means of a high impedance voltmeter, the reference electrode consisted of a nickel wire dipped in the cup of a Luggin tube filled with identical solution to that used in the cell. The tip of the Luggin tube was placed 0.5–1 mm from the cathode surface. Before each run N_2 gas was bubbled in the solution to eliminate dissolved oxygen. Solution used were made of equimolar amounts of $K_3Fe(CN)_6$ and $K_4Fe(CN)_6$ dissolved in 2N NaOH. Ferricyanide concentrations used were 0.025 M, 0.05 M and 0.1 M. Concentrations of ferricyanide and ferrocyanide were checked by iodometry and $KMnO_4$ titration respectively [18]. All solutions were prepared using distilled water and A.R. grade chemical. All experiments were carried out at 25±1°C. Each experiment was carried out twice, the average deviation in the limiting current between the two experiments was about 3.5%. Solution density and viscosity needed for data correlation were determined using a density bottle and an Ostwald viscometer, respectively [19]. The diffusivity of ferricyanide ion was obtained from the literature [11,20].

During each run the rotation speed of the motor and the cathode was controlled by a variac and was measured by an optical tachometer. During runs with superimposed solution flow, solution velocity was controlled by means of a by pass and was measured by a graduated cylinder and a stopwatch. The characteristics of the screens used as cathode are shown in Table 1. For the present square-weave wire mesh, the interfacial area per unit volume of the screen (specific surface area) is given by [21–23]

$$a_0 = \frac{2\pi m^2 d_w L}{\delta} \quad (5)$$

where

$$L = \left(\frac{d_w^2}{4} + \frac{1}{m^2}\right)^{0.5} \quad (6)$$

Table 1
Specifications of screens used in the present work

Mesh number, wire/inch	10	14	20	30
Wire diameter (cm)	0.071	0.049	0.039	0.027
Aperture (cm)	0.186	0.132	0.088	0.059
Screen thickness (cm)	0.142	0.098	0.078	0.054
Specific surface area (cm^{-1})	12.48	17.48	25.04	37.61
Area of single screen cathode, A, (cm^2)	34.3	33.6	38.3	39.8

The cathode area A was obtained by multiplying the screen volume by a_0. The screen volume is equal to the projected screen area multiplied by the screen thickness. Single screen thickness was taken twice the wire diameter [21–23].

Stainless steel screens were coated with a thin layer of nickel as described elsewhere [24]. Nickel was deposited on stainless steel screens from a solution containing 240 g/l nickel chloride and 86 cm^3 conc. HCl (Sp. gravity=1.18) under the following conditions:

Current density=3A/dm^3; temperature=25°C; time=5 min. Before plating, the stainless steel screen was immersed in the plating solution for 15 min without current to remove the oxide film. Nickel plating for 5 min had a negligible effect on wire diameter and other screen properties as revealed by the microscope.

3. Results and discussions

Polarization curves with a well defined limiting current plateau were obtained under different conditions. The limiting current obtained from these polarization curves was used to calculate the mass transfer coefficient according to the equation

$$K = \frac{I}{ZFAC} \tag{7}$$

Fig. 2 shows the effect of rotation speed on the mass transfer coefficient at rotating screens of different mesh number. The mass transfer coefficient increases with the rotational speed to a power which agrees well with the value 0.5 found in case of solid rotating discs, the higher the mesh number the higher the rate of mass transfer at the rotating screen disc.

Fig. 3 shows a comparison between the present data and previous data obtained using solid rotating discs in the laminar flow regime ($Re<2\times10^5$) [25]. Fig. 3 shows that for a given rotational Reynolds number the rate of mass transfer at rotating screen discs is much higher than that at rotating discs whether rotating in infinite medium [15] or rotating in a limited space [16,17] under laminar flow conditions. Fig. 3 also shows a comparison between the present data and turbulent flow mass transfer data at solid rotating disc [11]. Fig. 3 shows that the magnitude of Sh calculated from the equation representing turbulent flow at solid rotating disc (Eq. (4)) lies within the range of the present data i.e turbulent flow and thus enhanced transport can be achieved at lower Re at rotating screen disc than the traditional solid rotating disc.

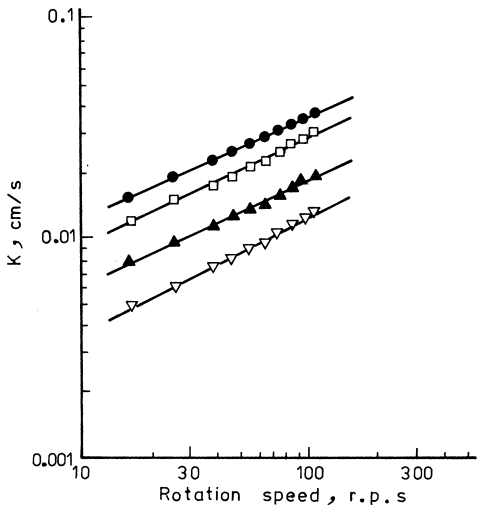

Fig. 2. Effect of screen rotation speed on the mass transfer coefficient ferricyanide concentration =0.1 M (Sc=2383) Screen mesh number: 10 (▽); 14 (▲); 20 (□); 30 (●).

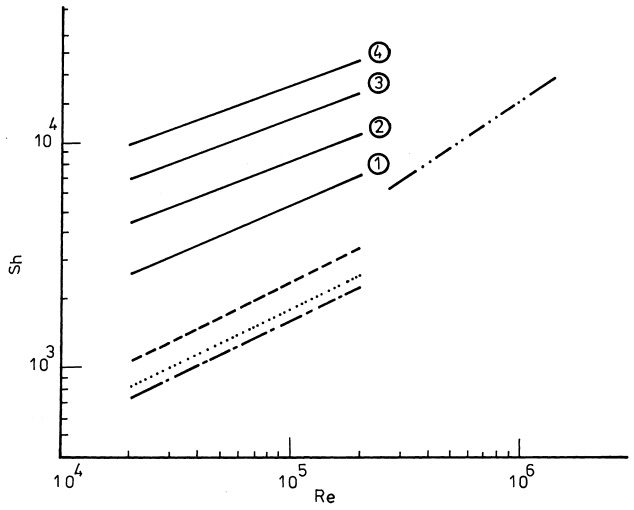

Fig. 3. Effect of Re on Sh at different rotating screens in comparison with the rotating disc electrode Sc=2290. Screen mesh number: 10 (1); 14 (2); 20 (3); 30 (4); Rotating disc [15] (- - -); rotating disc [17] (–··–); rotating disc [17] (···); rotating disc under turbulent flow [11] (–·–·–).

In order to assist in explaining the mass transfer behaviour of rotating screen disc, visual observation of the flow pattern at rotating screen disc was carried out using polystyrene granules as a tracer. Observations revealed the presence of rotational (swirl) motion of the solution and an axial flow toward the rotating screen disc. The axial flow is diverted in the radial direction at the surface of the rotating screen disc by virtue of the centrifugal force developed by the surface drag. It seems that the overall flow pattern at rotating screens is similar to that at discs rotating in a limited space [16]. The high mass transfer coefficient at rotating screens compared to rotating discs may be attributed to the turbulence promoting ability of the rotating screen. Turbulence is probably generated as the radial flow moves past the screen wires perpendicular to the flow. Turbulence could also be generated when the wires of the rotating screen move through the solution as a result of boundary layer separation in the wakes of the moving wires. The higher rate of mass transfer at rotating screens compared to rotating discs may also be attributed to the successive buildup and decay of the boundary layer formed as the radially flowing solution moves past the

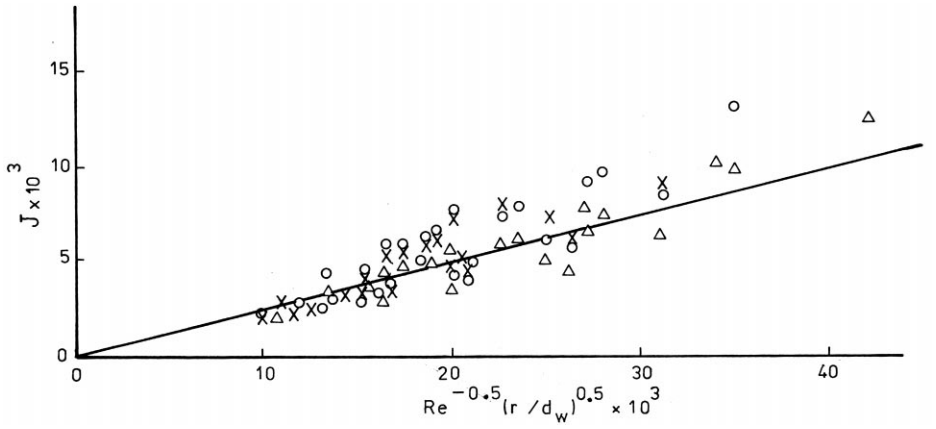

Fig. 4. Overall mass transfer correlation at rotating screens. Sc: 2290 (×); 2383 (△); 2653 (○).

screen wires; i.e the average hydrodynamic boundary layer and diffusion layers thickness in case of rotating screens are much less than their counterparts at rotating discs where the hydrodynamic boundary layer and diffusion layer extend over the disc radius.

The increase in the mass transfer coefficient with increasing the mesh number of the rotating screen may be attributed to the increase in the number of turbulence promoting elements.

3.1. Data correlation using the surface renewal model

Higbie's surface renewal theory [26] assumes that mass transfer takes place through the movement of a packet of solution with initial concentration C from the bulk to the mass transfer surface. After an interfacial residence time t_o during which the concentration of the reactant in the packet decreases, it returns to the solution bulk. Mass transfer from the packet to the mass transfer surface takes place by unsteady state diffusion. For a sufficiently short time t_o the mass transfer coefficient is given by

$$K = 2\left(\frac{D}{\pi t_0}\right)^{0.5} \tag{8}$$

Ruckenstein [27] extended the surface renewal model to turbulent flow mass transfer. He interpreted the surface renewal mechanism as a laminar flow of a packet of the solution for a short distance x_0 along the mass transfer surface followed by mixing with the solution bulk. The process is repeated after each length x_0. For high Sc Ruckenstein derived the equation

$$K \propto D\left(\frac{V}{\nu x_0}\right)^{0.5}\left(\frac{\nu}{D}\right)^{0.33} \tag{9}$$

In case of rotating screens the repeated growth and decay of the hydrodynamic boundary layer as the solution flows radially past the screen wires suggests applying the Ruckenstein model. It is reasonable to assume that x_0 is equal to the screen wire diameter (d_w); the linear velocity V of the solution at the rotating screen surface is given by

$$V = \omega r \tag{10}$$

Substituting for V and x_0 in Eq. (9) by ωr and d_w, respectively, then multiplying both sides of the equation by r we get the equation

$$\mathrm{Sh} = a\,\mathrm{Re}^{0.5}\,\mathrm{Sc}^{0.33}\left(\frac{r}{d_w}\right)^{0.5} \tag{11}$$

Dividing both sides by ($\mathrm{Re}\,\mathrm{Sc}^{0.33}$)

$$J = a\,\mathrm{Re}^{-0.5}\left(\frac{r}{d_w}\right)^{0.5} \tag{12}$$

Fig. 4 shows that the present data for the conditions $52\,500 < \mathrm{Re} < 340\,000$; $2290 < \mathrm{Sc} < 2650$ and $35.7 < r/d_w < 92.6$ fit the equation:

$$J = 0.26\,\mathrm{Re}^{-0.5}\left(\frac{r}{d_w}\right)^{0.5} \tag{13}$$

with an average deviation of ±12.4%. Attempts to obtain an empirical correlation in terms of other screen parameters such as the hydraulic radius did not produce a better correlation.

Fig. 5 shows the mass transfer behaviour of rotating fixed bed of closely packed horizontal screens, the number of screens ranged from 1 to 7; the data shows that the mass transfer coefficient decreases below the single screen value by an amount ranging from 20 to 43.6% depending on rotation speed, bed thickness and mesh number. The decrease is probably caused by the local decrease of reactant concentration and eddy damping inside the bed, and the decrease in the active area of the screens as a result of the contact between the screens forming the bed. A similar decrease was observed in case of stationary screen beds stirred by single phase flow [23] and gas sparging [7].

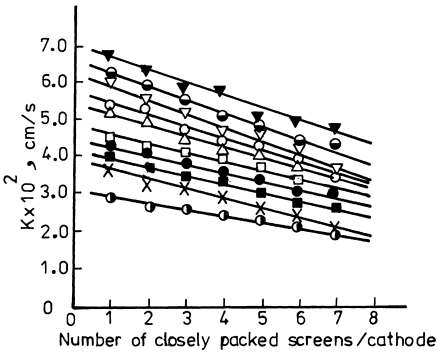

Fig. 5. Effect of number of closely packed screens per rotating array (rpm) on the mass transfer coefficient at different rotation speeds. Ferricyanide concentration =0.025 M (Sc=2290). Screen mesh number=20: 1040 (▼); 930 (○); 830 (▽); 730 (○); 540 (□); 450 (●); 370 (■); 250 (×); 160 (◑).

Fig. 6 shows the effect of screen separation on the mass transfer coefficient at an array of two spaced rotating screens, the mass transfer coefficient decreases with decreasing screen separation probably because of the unfavourable interaction of the flow induced by the upper and lower rotating screens which diminishes the radial flow velocity at the lower surface of the upper screen and the upper surface of the lower screen.

Fig. 7 shows the effect of superimposed solution flow on the rate of mass transfer at a single rotating screen, the flow velocities ranged from 0.4 to 5.7 cm/s ($180<Re_f<25\,000$. At low solution velocities in the range 0.4–2 cm/s ($180<Re_f<893$), the mass transfer coefficient increases slightly over the rotating screen value with increasing Re_f according to the equation:

$$Sh = a_l\, Re_f^{0.135} \tag{14}$$

The contribution of superimposed flow becomes more pronounced at $Re_f=1095$. It seems that superimposed flow con-

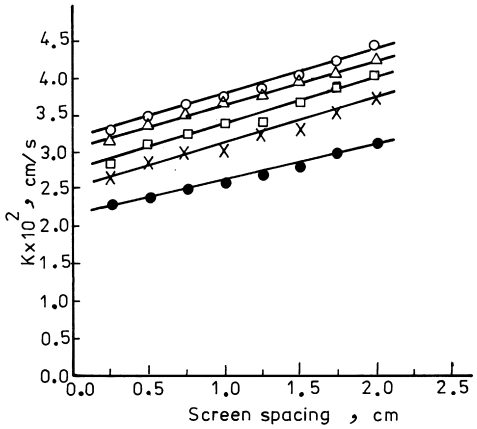

Fig. 6. Effect of screen spacing on the mass transfer coefficient at a rotating array (rpm) composed of two separated screens. Ferricynanide concentration =0.025 M (Sc=2290). Screen mesh number=30: 1040 (○); 830 (△); 630 (□); 450 (×); 250 (●).

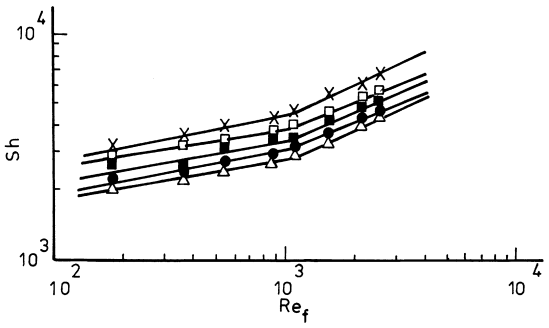

Fig. 7. Effect of superimposed axial flow on the rate of mass transfer at a single rotating screen (rpm). Ferricyanide concentration =0.025 M (Sc=2290); Screen mesh number =10: 1040 (×); 830 (□); 630 (■;; 450 (●); 250 (△).

tributes to enhancing the rate of mass transfer at the rotating screen via eddy generation downstream of the rotating screen [28,29] and the local increase in solution velocity (jet like flow) as the solution passes through the screen openings. For $Re_f>1095$, Sh increases with Re_f at a given screen rotation speed according to the equation:

$$Sh = a_2 Re_f^{0.38} \tag{15}$$

The exponent 0.38 is in a good agreement with the values 0.358 and 0.373 obtained by authors who studied the effect of solution flow on the rate of mass transfer at horizontal stationary screens [30].

The high mass transfer rates observed in the present work at rotating screens along with their high specific area qualify them for building high space time yield catalytic and electrochemical reactors suitable for conducting diffusion controlled reactions, e.g. electrosynthesis and recovery of heavy metals from industrial waste water. The continuous operation of such reactor at low feed rates would give a high degree of conversion per pass in view of the high residence time and the high rate of mass transfer. The reactor can be extended vertically by increasing the number of separated screens or arrays of closely packed screens mounted on the rotating shaft with a consequent decrease in floor space and capital costs. The reactor can be used as undivided or divided electrochemical reactor by using porous diaphragm or ion exchange membrane. The mass transfer coefficient needed for the design and operation of the reactor could be approximately calculated from the single screen equation (Eq. (13)) with due allowance to the deviation from the single screen behaviour as a result of using electrodes made of closely spaced screens.

4. Nomenclature

a_0	screen specific surface area
a_1, a_2	constants
A	surface area of the cathode
C	ferricyanide concentration

d_w screen wire diameter
d diameter of the cell container
D diffusivity of ferricyanide ion.
F Faraday's constant
I_L limiting current
K mass transfer coefficient
L defined by Eq. (6)
m mesh number (wires/cm)
V linear velocity of the rotating disc ($V=\omega r$).
V_f superimposed solution velocity
r disc radius
rps revolutions per second
Z number of electrons involved in the reaction
J mass transfer J factor (J=St. $Sc^{0.66}$)
Re Reynolds number of rotating screen($\rho\omega r^2/\mu$)
Re_f Reynolds number of superimposed flow($\rho V_f d/\mu$)
Sc Schmidt number ($\mu/\rho D$)
Sh Sherwood number (Kr/D)
St Stanton number (K/ωr)
μ solution viscosity
ρ solution density
ω angular velocity of the screen [$\omega=2\pi$(rps)]
δ screen thickness

References

[1] J. Cano, U. Bohm, Chem. Eng. Sci. 32 (1977) 213.
[2] A. Stork, P.M. Robertson, N. Ibl, Electrochim. Acta. 24 (1979) 373.
[3] R. Alkire, P.K. Ng, J. Electrochem. Soc. 124 (1977) 1220.
[4] R.E. Sioda, Electrochim. Acta 22 (1977) 439.
[5] L. Coppola, O.N. Cavatorta, U. Bohm, J. Appl. Electrochem. 19 (1989) 100.
[6] M. Zaki, I. Nirdosh, G.H. Sedahmed, The Can. J. Chem. Eng. 75 (1997) 333.
[7] F.A. Katkout, A.A. Zatout, H.A. Farag, G.H. Sedahmed, The Can. J. Chem. Eng. 66 (1988) 497.
[8] G.H. Sedahmed, The Can. J. Chem. Eng. 74 (1996) 487.
[9] M. Zaki, Y.A. El-Taweel, A.A. Zatout, M.Z. El-Abd, G.H. Sedahmed, J. Electrochem. Soc. 138 (1991) 430.
[10] G.H. Sedahmed, M.Z. El-Abd, A.A. Zatout, Y.A. El-Taweel, M.M. Zaki, J. Electrochem. Soc. 141 (1994) 437.
[11] J.R. Selman, C.W. Tobias, Adv. Chem. Eng. 10 (1978) 211.
[12] E.B. Cavalcanti, F. Coeuret, in: Proceeding Of The 4th International Workshop On Electrochemical Flow Measurements, March 1996, Lahnstein, Germany.
[13] A.R. Despic, M.N. Konjovic, M. Mitrovic, J. Appl. Electrochem. 7 (1977) 545.
[14] T. Sasaki, T. Ishikawa, Electrochim. Acta 31 (1986) 745.
[15] V.G. Levich, Physicochemical Hydrodynamics, Prentice Hall, Englewood Cliffs, NJ, 1962.
[16] G.D. Lehmkuhl, J.L. Hudson, Chem. Eng. Sci. 26 (1971) 1601.
[17] S. Langlosis, J.O. Nanzer, F. Coeuret, J. Appl. Electrochem. 19 (1989) 736.
[18] A.I. Vogel, A Textbook of Quantitative Inorganic Analysis, 3rd Edition, Longman, London, 1961.
[19] A. Findlay, J.K. Kitchener, Practical Physical Chemistry, Longmans, London, 1965.
[20] M. Eisenberg, C.W. Tobias, C.R. Wilke, J. Electrochem. Soc. 103 (1956) 413.
[21] J.C. Armour, J.N. Cannon, AIChE J. 14 (1968) 415.
[22] P.M. Lessner, F.R. McLarnon, J. Winnick, E.J. Cairns, J. Appl. Electrochem. 22 (1992) 927.
[23] C.N. Satterfield, D.H. Cortez, Ind. Eng. Chem. Fundam. 9 (1970) 613.
[24] The Canning Handbook Surface Finishing Technology, Canning plc., Birmingham, 1982, p. 347.
[25] A.C. Riddiford, Advances in Electrochem. and Electrochem. Eng. 4 (1966) 47.
[26] R. Higbie, Trans. Am. Inst. Chem. Engrs 31 (1935) 365.
[27] E. Ruckenstein, Chem. Eng. Sci. 7 (1958) 265.
[28] J.G. Knudsen, D.L. Katz, Fluid Dynamics and Heat Transfer, McGraw Hill, New York, 1958.
[29] J.R. Bourne, M. Lips, The Chem. Eng. J 47 (1991) 155.
[30] T.Z. Fahidy, Principles of Electrochemical Reactor Analysis, Elsevier, New York, 1985, p. 83.